

Articles

Evidence for Intramolecular NH- -S Hydrogen Bonds from $^2\text{H-NMR}$ Spectroscopy of Reduced-Rubredoxin Model Fe(II) Complexes with Bidentate Peptide Ligands

Norikazu Ueyama, Wei-Yin Sun, and Akira Nakamura*

Department of Macromolecular Science, Faculty of Science, Osaka University, Toyonaka, Osaka 560, Japan

Received February 19, 1992

The $^1\text{H-NMR}$ signals of Cys C_βH_2 of reduced rubredoxin models, $(\text{NEt}_4)_2[\text{Fe}(\text{Z-cys-Pro-Val-cys-OMe})_2]$ (**2**), $(\text{NEt}_4)_2[\text{Fe}(\text{Z-cys-Pro-Leu-cys-OMe})_2]$ (**3**), and $(\text{NEt}_4)_2[\text{Fe}(\text{-cys-Pro-Leu-cys-Gly-Val-OMe})_2]$ (**4**), were isotropically shifted to lower field and widely separated in the range 150–250 ppm in acetonitrile- d_3 . This is ascribed mainly to relative positions of two sets of Cys $\text{C}_\beta\text{H}_A\text{H}_B$ protons in a macrocyclic peptide-chelating ring of Cys-X-Y-Cys/Fe(II). The presence of four isotropically shifted amide N^2H signals in the $^2\text{H-NMR}$ spectrum of complex **4** gives direct evidence for the formation of $\text{N}^2\text{H- -S}$ hydrogen bonds which consist of two strong bonds and one weak bond in the macrocyclic ring of the Cys-Pro-Y-Cys (Y = Val or Leu) fragment as in those of complexes **2** and **3** and one solvent-dependent bond in the hairpin turn of the Cys-Gly-Val fragment as suggested by the X-ray analysis of the active site of rubredoxin. Energy-minimized calculation of **4** indicates that the bulkiness of the Gly-Val fragment next to the Cys-Pro-Leu-Cys chelating fragment results in exclusive formation of a δ isomer. The result is in good agreement with the conclusion derived from the $^2\text{H-NMR}$ spectrum of complex **4**.

Introduction

Rubredoxin has a simple structure in the active site which contains one Fe ion surrounded by four cysteine thiolate ligands of two Cys-X-Y-Cys fragments.¹ Studies on the distorted geometry of the oxidized or reduced iron center have been carried out using Raman² and MCD³ spectroscopic methods. The tetragonally distorted tetrahedral structure has been indicated for the Ni-substituted active center of rubredoxin.⁴ Recently, the comparison of the electronic spectra of $[\text{Fe}(\text{S-2-(Ph)C}_6\text{H}_4)_4]^{2-}$ with those of rubredoxin has revealed the same slight distortion.⁵

The spectroscopic and theoretical studies of cysteine-containing peptide model complexes such as $[\text{Fe}^{\text{III}}(\text{Z-cys-Pro-Leu-cys-OMe})_2]^-$ and $[\text{Fe}^{\text{III}}(\text{Z-cys-Thr-Val-cys-OMe})_2]^-$, as models of oxidized *Clostridium pasteurianum* rubredoxin have revealed that the slight distortion of the $[\text{Fe}(\text{S-cys})_4]^-$ core from D_{2d} to C_2 is ascribed to the eclipsed Fe-S torsion angles by the Cys(1)-X-Y-Cys(2) chelation.^{6,7} The eclipsed conformation of the Fe-S Cys portion provides two kinds of Fe-S bonds among the four bonds with different π -bonding characters.

High-spin Fe(II) complexes have been reported to exhibit isotropically shifted $^1\text{H-NMR}$ signals, e.g. octahedral (porphy-

rinato)iron(II) complexes⁸ and tetrahedral $[\text{Fe}^{\text{II}}(\text{SEt})_4]^{2-}$.⁹ The chelation of the Z-Cys-X-Y-Cys-OMe ligand to Fe(II) or Co(II) has been established by CD and MCD spectra in Me_2SO or acetonitrile.^{10,11} Recently, Kurtz et al. have reported the $^1\text{H-NMR}$ spectra of reduced *Desulfovibrio gigas* rubredoxin.¹² They found four sets of isotropically shifted Cys C_βH_2 signals which were widely separated in the range 140–240 ppm.

In order to investigate the role of a fragment, Cys-Gly-A (A = Val or Tyr), connecting with a Cys-X-Y-Cys chelating fragment in the active site of rubredoxin, we synthesized $(\text{NEt}_4)_2[\text{Fe}(\text{Z-cys-Pro-Leu-cys-Gly-Val-OMe})_2]$. The nature of hydrogen bonds in the model complex can be inferred by the correct assignment of the $^1\text{H-NMR}$ signals by using $^2\text{H-NMR}$ spectra utilizing specific isotropically shifted peaks. The position of these assigned signals is expected to reveal the important role of NH- -S hydrogen bonds around the active site of rubredoxin.

Experimental Section

Materials. All operations were carried out under argon atmosphere. Acetonitrile, methanol- d_1 , tetrahydrofuran (THF), and all other solvents were purified by distillation before use. $(\text{NEt}_4)_2[\text{FeBr}_4]$ was prepared by the literature method.¹³

Synthesis of Z-Cys-Gly-Val-OMe. Z-Cys(Acm)-Gly-Val-OMe (Z = benzyloxycarbonyl; Acm = acetamidomethyl) was synthesized by the mixed anhydride method reported in the literature.¹⁴ To a solution of Z-Cys(Acm)-Gly-Val-OMe (1.0 g, 2.0 mmol) in 10 mL of methanol was

- (1) (a) Lovenberg, W.; Sobel, B. E. *Proc. Natl. Acad. Sci. U.S.A.* **1965**, *54*, 193. (b) Watenpaugh, K. D.; Sieker, L. C.; Herriott, J. R.; Jensen, L. H. *Acta Crystallogr., Sect. B* **1973**, *29*, 943. (c) Eaton, W. A.; Lovenberg, W. *Iron-sulfur-Proteins*; Lovenberg, W., Ed.; Academic: New York, 1973; Vol. II, pp 131–162.
- (2) Yachandra, V. K.; Hare, J.; Moura, I.; Spiro, T. G. *J. Am. Chem. Soc.* **1983**, *105*, 6455.
- (3) Ulmer, D. D.; Holmquist, B.; Vallee, B. L. *Biochem. Biophys. Res. Commun.* **1973**, *51*, 1054.
- (4) Kowal, A. T.; Zambrano, I. C.; Moura, I.; Moura, J. J. G.; LeGall, J.; Johnson, M. K. *Inorg. Chem.* **1988**, *27*, 1162.
- (5) (a) Lowercase letter, e.g. *cys*, refers to a coordinating amino acid residue. (b) Gebhard, M. S.; Koch, S. A.; Millar, M.; Devlin, F. J.; Stephens, P. J.; Solomon, E. I. *J. Am. Chem. Soc.* **1991**, *113*, 1640.
- (6) Nakata, M.; Ueyama, N.; Terakawa, T.; Nakamura, A. *Bull. Chem. Soc. Jpn.* **1983**, *56*, 3647.
- (7) Ueyama, N.; Sugawara, T.; Tatsumi, K.; Nakamura, A. *Inorg. Chem.* **1987**, *26*, 1978.

- (8) La Mar, G. N.; Walker, F. A. In *The Porphyrins*; Dolphin, D., Ed.; Academic Press: New York, 1979; Vol. 4, p 61.
- (9) Hagen, K. S.; Watson, A. D.; Holm, R. H. *J. Am. Chem. Soc.* **1983**, *105*, 3905.
- (10) Ueyama, N.; Nakata, M.; Fuji, M.; Terakawa, T.; Nakamura, A. *Inorg. Chem.* **1985**, *24*, 2190.
- (11) Nakata, M.; Ueyama, N.; Terakawa, T.; Nakamura, A.; Nozawa, T.; Hatano, M. *Inorg. Chem.* **1983**, *22*, 3028.
- (12) Werth, M. T.; Kurtz, D. M., Jr.; Moura, I.; LeGall, J. *J. Am. Chem. Soc.* **1987**, *109*, 273.
- (13) Gill, N. S.; Taylor, F. B. *Inorg. Synth.* **1967**, *9*, 136.
- (14) Ueyama, N.; Nakata, M.; Nakamura, A. *Bull. Chem. Soc. Jpn.* **1985**, *58*, 464.

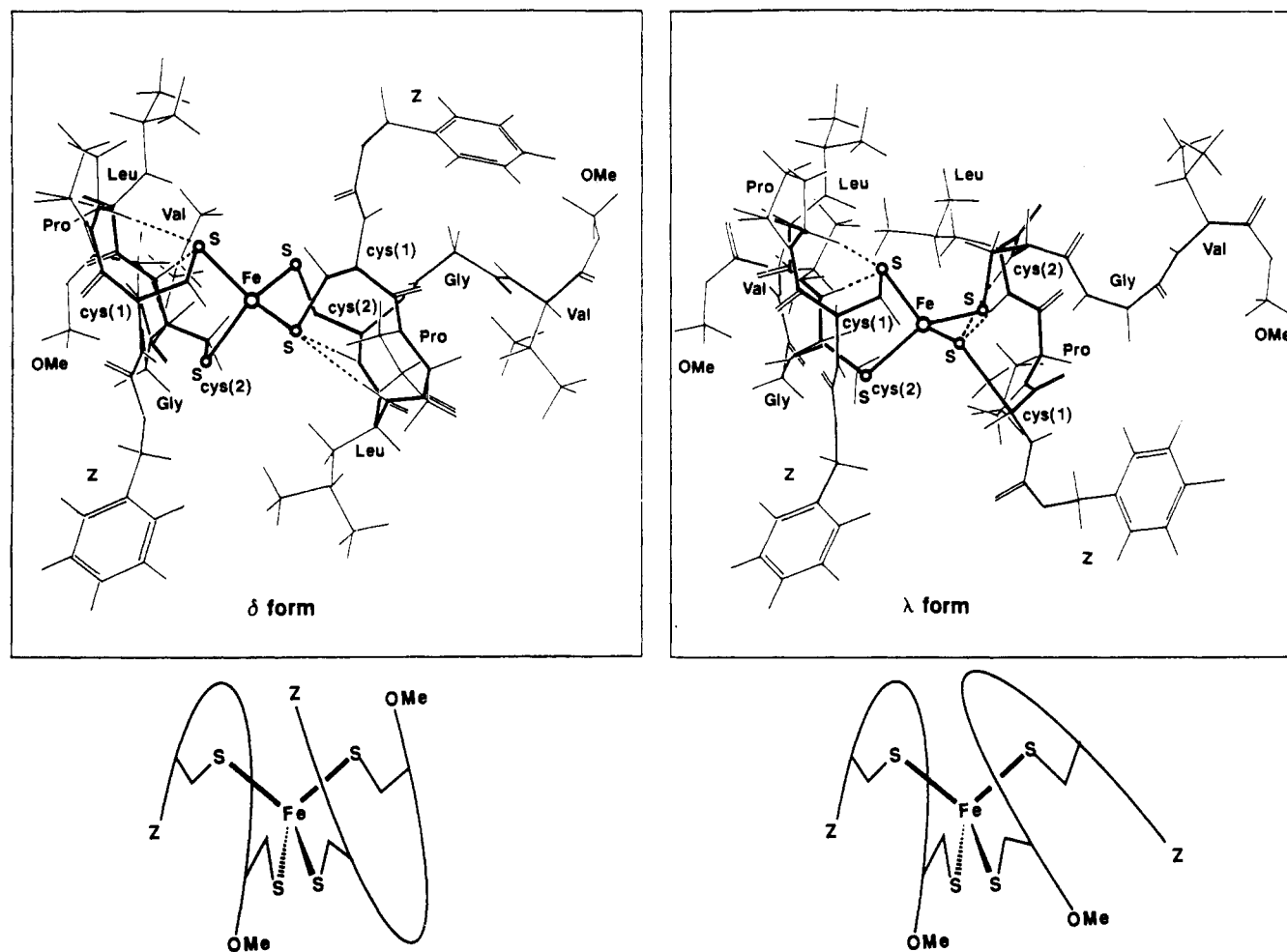


Figure 1. Schematic drawing for the two proposed isomers (δ and λ) of $[\text{Fe}^{\text{II}}(\text{Z-cys-Pro-Leu-cys-Gly-Val-OMe})_2]^{2-}$ (4). Graphic outputs of these conformers were obtained by using BIOGRAF energy-minimum calculations.

added a solution of AgOCOCF_3 (1.3 g, 6.0 mmol) in 10 mL of methanol.¹⁵ The mixture was stirred overnight. A colorless precipitate was collected by filtration and dried in vacuo to give a peptide-Ag(I) complex in 99% yield (1.5 g). Anal. Calcd for $\text{C}_{21}\text{H}_{26}\text{N}_3\text{O}_8\text{SAg}_2\text{F}_3[\text{Z-cys}(\text{Ag})\text{-Gly-Val-OMe}][\text{AgOCOCF}_3]$: C, 33.49; H, 3.48; N, 5.58. Found: C, 33.30; H, 3.47; N, 5.54.

Hydrogen sulfide gas was introduced into a solution of $[\text{Ag}_2(\text{OCOCF}_3)_2(\text{Z-cys-Gly-Val-OMe})]$ (300 mg, 0.4 mmol) in methanol (40 mL) for 20 min. Black precipitates were removed by filtration and the filtrate was concentrated under reduced pressure. A white powder was obtained and washed with fresh diethyl ether and dried in vacuo.

Synthesis of Z-Cys(Acm)-Pro-Leu-Cys(Acm)-Gly-Val-OMe. Boc-Cys(Acm)-Gly-Val-OMe (Boc = *tert*-butyloxycarbonyl) was synthesized by the same procedure as described for Z-Cys(Acm)-Gly-Val-OMe.¹⁴ Z-Cys(Acm)-Pro-Leu-OPac (Pac = phenacyl) was prepared stepwise by the mixed anhydride method according to the literature.¹⁶

Zinc powder (10 g) was added to a 90% acetic acid solution of Z-Cys(Acm)-Pro-Leu-OPac (2.0 g, 3.0 mmol). The mixture was stirred for 1 h at 0 °C and for 3 h at room temperature. After the excess zinc was removed by filtration, the colorless filtrate was concentrated in vacuo. The residue was dissolved in water, acidified by citric acid, and extracted with ethyl acetate. The ethyl acetate layer collected was concentrated under reduced pressure to give a colorless oily residue. The oily material was dissolved in DMF (4 mL), and a mixture of $\text{HCl}\cdot\text{H-Cys-Gly-Val-OMe}$ (1.2 g, 3.0 mmol) and triethylamine (0.42 mL, 3.0 mmol) in DMF (3 mL) was added to the solution, before HOBt (1-hydroxybenzotriazole) was added (609 mg). DCC (*N,N'*-dicyclohexylcarbodiimide) (774 mg) was added to the solution at -5 °C. The reaction mixture was stirred at room temperature for 4 days and purified by the usual procedures to give a white powder, which was reprecipitated from chloroform and diethyl ether in 10% yield. Anal. Calcd for $\text{C}_{39}\text{H}_{60}\text{N}_8\text{O}_{11}\text{S}_2[\text{Z-}$

$\text{cys}(\text{Acm})\text{-Pro-Leu-cys}(\text{Acm})\text{-Gly-Val-OMe}]$: C, 53.17, H, 6.86; N, 12.72; S, 7.28. Found: C, 52.79; H, 6.79; N, 12.60; S, 7.29.

Synthesis of $[\text{Ag}_4(\text{OCOCF}_3)_2(\text{Z-cys-Pro-Leu-cys-Gly-Val-OMe})]$. A solution of Z-Cys(Acm)-Pro-Leu-Cys(Acm)-Gly-Val-OMe (23 mg, 0.026 mmol) in methanol (2 mL) and AgOCOCF_3 (29 mg, 0.13 mmol) in methanol (2 mL) was mixed and stirred overnight. The solvent was removed in vacuo and the residue was washed with diethyl ether several times to give the Ag(I) complex. Anal. Calcd for $\text{C}_{37}\text{H}_{48}\text{N}_6\text{O}_{13}\text{S}_2\text{Ag}_4\text{F}_6[\text{Z-cys}(\text{Ag})\text{-Pro-Leu-cys}(\text{Ag})\text{-Gly-Val-OMe}][\text{Ag}_2(\text{OCOCF}_3)_2]$: C, 31.68; H, 3.73; N, 6.20. Found: C, 31.87; H, 3.47; N, 6.03.

$(\text{NEt}_4)_2[\text{Fe}(\text{S-}t\text{-Bu})_4]$. $(\text{NEt}_4)_2[\text{FeBr}_4]$ (1.9 g, 3.0 mmol) and NaS-*t*-Bu (1.7 g, 14.8 mmol) were mixed in 10 mL of acetonitrile at room temperature. The solution turned purple. After removal of precipitates by filtration, diethyl ether was added to the filtrate and the solution was allowed to stand at -5 °C for 24 h. The precipitates were collected with filtration and recrystallized from THF and diethyl ether. Colorless crystals were obtained in a 20% yield. Anal. Calcd for $\text{C}_{32}\text{H}_{76}\text{N}_2\text{FeS}_4\{(\text{NEt}_4)_2[\text{Fe}(\text{S-}t\text{-Bu})_4]\}$: Fe, 8.30. Found: Fe, 8.81. The complex was extremely sensitive to air and water as reported for $(\text{NEt}_4)_2[\text{Fe}(\text{SEt})_4]$.⁹ UV-visible absorption (in acetonitrile): ϵ_{max} 290 nm ($7400 \text{ M}^{-1} \text{ mol}^{-1}$) and 340 nm ($3000 \text{ M}^{-1} \text{ mol}^{-1}$). ¹H-NMR (in acetonitrile-*d*₃, 25 °C): 23 ppm (S-*t*-Bu). The signal persists at 23 ppm even with addition of 10 equiv of *t*-BuSH. Also, the temperature-dependent isotropically shifted *t*-Bu signal obeys a Curie law as in the results reported for Co(II)-substituted stellacyanin.¹⁷ The results indicate a monomeric, high-spin Fe(II) structure for $[\text{Fe}^{\text{II}}(\text{S-}t\text{-Bu})_4]^{2-}$ in solution.

$(\text{NEt}_4)_2[\text{Fe}(\text{Z-cys-Gly-Val-OMe})_4]$ (1). The complex was synthesized by a ligand-exchange reaction of $(\text{NEt}_4)_2[\text{Fe}(\text{S-}t\text{-Bu})_4]$ (14 mg, 0.02 mmol) and Z-Cys(SH)-Gly-Val-OMe (36 mg, 0.08 mmol) in acetonitrile (10 mL) and obtained as a brownish powder. The integral ratio (CH_3 in NEt_4 vs OMe) of ¹H-NMR methyl signals was ca. 2.0.

(15) Deprotection of Acm group by using AgOCOCF_3 as well as HgCl_2 .

(16) Sun, W. Y.; Ueyama, N.; Nakamura, A. *Inorg. Chem.* 1991, 30, 4026.

(17) Dahlin, S.; Reinhammar, B.; Angstrom, J. *Biochemistry* 1989, 28, 7224.

(NEt₄)₂[Fe(Z-cys-Pro-Val-cys-OMe)₂]²⁻ (2). (NEt₄)₂[Fe(S-*t*-Bu)₄]²⁻ (46 mg, 0.07 mmol) and Z-Cys(SH)-Pro-Val-Cys(SH)-OMe (75 mg, 0.14 mmol) were mixed in acetonitrile (15 mL) at ambient temperature. The solution was stirred at room temperature for 20 min. The purple solution was concentrated under reduced pressure. Addition of 10 mL of diethyl ether gave a brownish powder. The powder was collected by filtration, washed with diethyl ether, and dried in vacuo.

(NEt₄)₂[Fe(Z-cys-Pro-Leu-cys-OMe)₂]²⁻ (3). The complex was synthesized by the same method exemplified by the procedure for 2.

(NEt₄)₂[Fe(Z-cys-Pro-Leu-cys-Gly-Val-OMe)₂]²⁻ (4). Hydrogen sulfide gas was bubbled through a methanol solution of [Ag₄(OCOCF₃)₂(Z-cys-Pro-Leu-cys-Gly-Val-OMe)] (0.023 mmol) at room temperature for 20 min. After silver sulfide was removed with filtration, the filtrate was concentrated in vacuo. The residue was washed with fresh diethyl ether twice and gave a colorless powder.

A solution of (NEt₄)₂[Fe(S-*t*-Bu)₄]²⁻ (0.011 mmol) in acetonitrile (3 mL) was added to a THF (3 mL) solution of the SH-free Z-Cys-Pro-Leu-Cys-Gly-Val-OMe (0.022 mmol). The solution was concentrated to 1 mL volume under reduced pressure. Addition of diethyl ether resulted in precipitation of a light brown powder.

Preparation of N²H-Substituted Fe(II) Complexes. The amide N²H-substituted peptide ligands were obtained by the exchange of the SH-protected peptides with methanol-*d*₁. For example, Z-Cys-Gly-Val-OMe (17 mg) was dissolved in methanol-*d*₁ (1.5 mL) and stirred for about 15 min at 40 °C before the solvent was removed in vacuo. The same procedure was repeated several times to obtain the 94 ± 3% enriched peptides.

N²H-substituted Fe(II) complexes were synthesized from (NEt₄)₂[Fe(S-*t*-Bu)₄]²⁻ and the corresponding amide N²H-substituted peptide ligand by the same method described for the syntheses of complexes 1 and 2.

Physical Measurements. UV-visible and CD spectra were recorded on Jasco Ubest-30 and Jasco J-40 spectrophotometers using a 1-mm cell path. The values of ϵ and $\Delta\epsilon$ were given in units of M⁻¹ cm⁻¹. ¹H-NMR spectra were taken on a JEOL JNM-GX-500 spectrometer. Tetramethylsilane (TMS) was used as an external reference. The solvent ¹H-NMR signals were saturated using a single-pulse homogated decoupling mode. The irradiation of the solvent signals was performed with a multiple-frequency irradiation microprogram. To obtain each ¹H-NMR spectrum, an average of 10 000 transients was collected with a bandwidth of 200 kHz (400 ppm) using 16 384 data points. The recycle delay used was 0.1 s. The 61-MHz ²H-NMR spectroscopic measurements were carried out on a JEOL GSX-400 NMR spectrometer using SGBOMB (single pulse ¹H-NMR bilevel decoupling) mode and the peak at 4.7 ppm due to D₂O was used as an external reference. The recycle delay of 1.0 sec was used.

The energy difference between two isomers for [Fe^{II}(Z-cys-X-Y-cys-OMe)₂]²⁻ or [Fe^{II}(Z-cys-X-Y-cys-Gly-Val-OMe)₂]²⁻ was calculated using a BIOGRAF method.¹⁸ A Charmm force field was employed for the calculations. The potential energy consists of bonded terms (bond stretching, bond angle bending, dihedral angle torsion, and inversion terms), nonbonded terms (van der Waals, electrostatic, and hydrogen bond terms) and metal-binding terms (constraint of the geometry and charges of the ligands and Fe(II) ion). The FeS₄ core was constrained to a tetrahedral geometry, because only a slight distortion from *T_d* has been reported for the crystal structure of FeS₄ core in the active site of *C. pasteurianum* rubredoxin. The parameters of Fe(S-cys)₄ for the calculations were obtained from the crystallographic structure reported for [Fe^{II}(S₂-*o*-xyl)₂]²⁻ (*o*-xyl = *o*-xylene- α,α' -dithiolate): Fe-S, 2.35 Å; S-C, 1.82 Å; Fe-S-C, 109°. ¹⁹ The point charges of Fe(II) (+1.736), S (-0.5496), C (0.264), and H(0.225) estimated by the EHM0 calculations of [Fe^{II}(SCH₃)₄]²⁻ were employed as the values of Fe(II), Cys C _{β} H₂ and sulfur atoms.²⁰ No solvation was included because of the highly hydrophobic environment at the iron site of rubredoxin.

Results

Synthesis of Cysteine-Containing Fe(II) Complexes. The syntheses of Fe(II) model complexes of cysteine-containing peptides have previously been carried out using a Me₂SO solution

of [Fe(Me₂SO)₆]²⁺ and an excess of the corresponding cysteine-containing peptide.¹⁰ As a more convenient and versatile method for the synthesis of the cysteine-containing peptide Fe(II) complexes, we employed a ligand-exchange reaction between [Fe(S-*t*-Bu)₄]²⁻ and the corresponding peptide ligand. The reaction was completed by evaporation of *t*-BuSH under reduced pressure, a process which can be monitored by disappearance of *t*-Bu ¹H-NMR signals at 23 ppm at 25 °C.

The formations of mononuclear cysteine peptide-Fe(II) complexes were confirmed by absorption, CD and ¹H-NMR spectroscopy as described in the previous paper.¹⁶ [Fe^{II}(Z-cys-Pro-Val-cys-OMe)₂]²⁻ exhibits ligand-to-metal charge-transfer (LMCT) absorption maximum at 314 nm (4900) and CD transitions at 318 nm (-8.6) and 338 nm (4.4) in acetonitrile, which are very similar to those of [Fe^{II}(Z-cys-Pro-Leu-cys-OMe)₂]²⁻ in the same solvent.¹⁶

Energy-Minimum Calculations for Two Chelating Isomers. Two isomers can be formed theoretically in solution when the Cys-X-Y-Cys chelating peptide ligands coordinate to a tetrahedral Fe(II) ion with different orientation of peptide ligands. The δ form has the structure analogous to that of the chelating site of native rubredoxin.¹ The energy difference between the two diastereomers of [Fe^{II}(Z-cys-Pro-Leu-cys-OMe)₂]²⁻ obtained by the conformational energy-minimum calculation (BIOGRAF) method is quite small (below 4 kcal/mol). The energy-minimized conformers of the δ and λ isomers of complex 4 were also examined without constraint of NH- -S hydrogen bonding. Structures of two possible chelating diastereomers of [Fe^{II}(Z-cys(1)-Pro-Leu-cys(2)-Gly-Val-OMe)₂]²⁻ are shown in Figure 1. Two NH- -S hydrogen bonds intra-macrocyclic Cys(1)-Pro-Leu-Cys(2) chelating peptide ring, i.e. Leu-NH- -S-Cys(1) and Cys(2)-NH- -S-Cys(1), are formed naturally in both of the two isomers, as shown in Figure 1. The calculated total energy for the δ form was 166.9 kcal/mol while that for the λ form is 182.9 kcal/mol. Introduction of the bulky Gly-Val-OMe next to Cys(2) results in the steric congestion with the other Gly-Val-OMe group in the complex. The bulkiness in λ form contributes to a steric repulsion between both Pro-Leu side chains while in δ form there is no such repulsion (see Figure 1).

Isotropic Shifts of ¹H NMR Signals in Fe(II) Complexes of the Cysteine Peptides. Figure 2 shows the ¹H-NMR spectra of the various Fe(II) peptide complexes in the Cys C _{β} H₂ region in acetonitrile-*d*₃.^{9,12} The Cys C _{β} H₂ signals of (NEt₄)₂[Fe(Z-cys-Gly-Val-OMe)₄]²⁻ were observed as a single broad peak at 220 ppm at 30 °C (Figure 2a). The observation of the single peak indicates that the four Cys thiolate ligands of such a nonchelating peptide complex are equivalent and the CH_AH_B rotates freely without separation of H_A and H_B signals in the NMR time scale. Figures 2b-d show the analogous ¹H-NMR spectra of Fe(II) complexes containing peptide ligands, Z-Cys-Pro-Val-Cys-OMe (2), Z-Cys-Pro-Leu-Cys-OMe (3), and Z-Cys-Pro-Leu-Cys-Gly-Val-OMe (4). Complex 3 exhibits seven ¹H-NMR signals of Cys C _{β} H₂ at 257, 253, 244, 236, 190, 178 and 169 ppm (Figure 2c). The intensity of the signal at 178 ppm (signal 6c, 7c in Figure 2c) was twice that of the other signals (1c, 2c, 3c, 4c, 5c, or 8c). This indicates that the signal at 178 ppm is composed of two overlapping resonances (6c, 7c). Therefore, 3 gives eight Cys C _{β} H₂ signals in total. Complex 4 shows four broad signals of nearly equal intensity at 147, 200, 215, and 257 ppm (Figure 2d).²¹ The other two small signals are perhaps from trace amounts of the λ form. *T*₁ measurements for these signals were unsuccessful because of the small values (below 1 ms for all of signals in all the spectra shown in Figure 2).

Figure 3 shows Curie plots for the resonances of Figure 2. The fact that the Cys C _{β} H₂ signals are linear with 1/*T* and that the

(18) The graphic analysis was performed on a BIOGRAF molecular mechanics program supplied by Biodesign Inc., Pasadena, CA.

(19) Lane, R. W.; Ibers, J. A.; Frankel, R. B.; Papaefthymiou, G. C.; Holm, R. H. *J. Am. Chem. Soc.* 1977, 99, 84.

(20) Noodleman, L.; Norman, J. G., Jr.; Osborne, J. H.; Aizman, A.; Case, D. A. *J. Am. Chem. Soc.* 1985, 107, 3418.

(21) No ¹H-NMR signals were observed between 60 and 100 ppm for these complexes, indicating the absence of polynuclear species analogous to [Fe₄(SEt)₆]²⁺ and [Fe₄(SEt)₁₀]²⁺, which show signals in this region.²²

(22) Hagen, K. S.; Holm, R. H. *Inorg. Chem.* 1984, 23, 418.

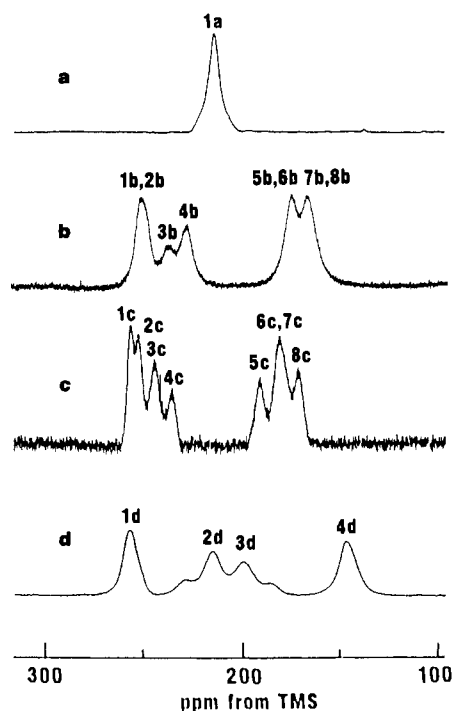


Figure 2. Cys $C_{\beta}H_2$ region of the 1H -NMR spectra of Cys-containing peptide-Fe(II) complexes in acetonitrile- d_3 at 30 °C: (a) $(NEt_4)_2[Fe^{II}-(Z-cys-Gly-Val-OMe)_4]$ (1); (b) $(NEt_4)_2[Fe^{II}(Z-cys-Pro-Val-cys-OMe)_2]$ (2); (c) $(NEt_4)_2[Fe^{II}(Z-cys-Pro-Leu-cys-OMe)_2]$ (3); (d) $(NEt_4)_2[Fe^{II}(Z-cys-Pro-Leu-cys-Gly-Val-OMe)_2]$ (4).

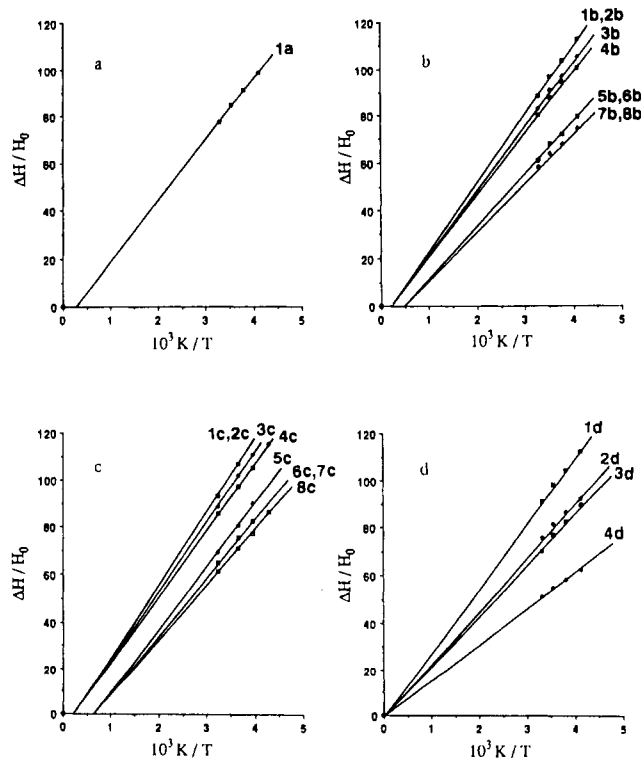


Figure 3. Curie plots against T^{-1} for the Cys $C_{\beta}H_2$ 1H -NMR signals shown in Figure 2: (a) $(NEt_4)_2[Fe^{II}(Z-cys-Gly-Val-OMe)_4]$ (1); (b) $(NEt_4)_2[Fe^{II}(Z-cys-Pro-Val-cys-OMe)_2]$ (2); (c) $(NEt_4)_2[Fe^{II}(Z-cys-Pro-Leu-cys-OMe)_2]$ (3); (d) $(NEt_4)_2[Fe^{II}(Z-cys-Pro-Leu-cys-Gly-Val-OMe)_2]$ (4).

extrapolation of the plots almost crosses the zero point of the $1/T$ axis indicates that the complexes are high spin and mononuclear in solution in the range of -30 to $+30$ °C. The results of Curie plots for the hyperfine shifted signals were listed in Table I in terms of slope and intercepts.

Table I. Slope and Intercepts of Curie Plots for Hyperfine-Shifted Signals Observed in 1H - and 2H -NMR Spectra Shown in Figures 2 and 4

assignment	complex	signal	slope ($\times 10^{-3}$ K)	intercept	
Cys $C_{\beta}H_2$	1	1a	24.2	-7.1	
		2	1b (2b)	27.5	-5.8
			3b	25.6	-4.7
			4b	24.7	-3.5
			5b (6b)	19.4	-10.7
			7b (8b)	17.9	-9.4
	3	1c (2c)	29.9	-6.5	
		3c	28.4	-6.1	
		4c	27.0	-5.2	
		5c	22.9	-16.6	
		6c (7c)	21.1	-14.9	
		8c	20.0	-13.7	
4	1d	27.6	~ 0		
	2d	22.7	~ 0		
	3d	21.7	~ 0		
	4d	15.6	~ 0		
N^2H	3	1'c	1.4	-1.7	
		2'c	1.0	~ 0	
		3'c	0.5	-2.0	
		4'c	0.2	-0.6	
		5'c	-0.6	1.9	
	4	1'd	1.2	-0.4	
		2'd	0.5	-0.9	
		3'd	-0.5	0.7	
		4'd	-1.1	0.2	

2H -NMR Spectra of N-Deuterated Peptide-Fe(II) Complexes.

The sample for 2H -NMR spectral measurements were prepared by reaction of $[Fe(S-t-Bu)_4]^{2-}$ with an N-deuterated SH-free peptide (see Experimental Section). Hence, only deuterated amide N^2H can be seen in our 2H -NMR spectra. The results are shown in Figure 4.

The monodentate cysteine-containing peptide complex, $(NEt_4)_2[Fe^{II}(Z-cys-Gly-Val-OMe)_4]$ exhibits two N^2H signals at 15.5 and 11.7 ppm in acetonitrile at 30 °C (Figure 4a). The small isotropic shifts observed for these signals suggest the absence of strong NH...S hydrogen bonds. In contrast, Figure 4c shows that $(NEt_4)_2[Fe^{II}(Z-cys-Pro-Leu-cys-OMe)_2]$ exhibits N^2H signals at 40.1, 34.7 ppm; 18.7, 13.1 ppm; and -4.1 ppm in acetonitrile at 30 °C.²³ The signals around 37 and 16 ppm were split into two indicating the presence of two isomers (about 1:1).^{16,24} $(NEt_4)_2[Fe^{II}(Z-cys-Pro-Val-cys-OMe)_2]$ shows similar N^2H signals at 40.2, 38.3 ppm; 13.4, 10.6 ppm, and -4.2, -6.2 ppm, but the ratio of the two isomers was not one (about 3:7) (Figure 4b). Furthermore, predominant formation of the one isomer was detected for $(NEt_4)_2[Fe^{II}(Z-cys-Pro-Leu-cys-Gly-Val-OMe)_2]$ as evidenced by the presence of one N^2H signal at each positions, 38.0, 19.5, -4.0, and -20.0 ppm (Figure 4d). The small signal at 40.5 ppm (see the insertion of signal 1'd shown in Figure 4d which was obtained by multiplying the transient signals by 10) was considered to be due to the presence of a slight amount of the λ form which is in agreement with the results of 1H -NMR spectroscopy as mentioned above.

The N^2H signals at 30 ~ 40 ppm of 2-4 were assigned to Cys(2) N^2H since $(NEt_4)_2[Fe^{II}(Z-cys(1)-Ala-Pro-cys(2)-OMe)_2]$ exhibits isotropically shifted N^2H signals at 24.5 and 22.8 ppm due to the formation of a Cys(2)- N^2H ...S-Cys(1) hydrogen bond in acetonitrile at 30 °C, and no other isotropically shifted

(23) The measurements of 2H -NMR spectra were carried out in a much wider region (-100 to $+400$ ppm), and no other exchangeable signals were detected.

(24) An Fe(II) complex of a tetradentate peptide ligand, *cis*-1,2-cyclohexylene-(CO-Cys-Pro-Leu-Cys-OMe)₂ where only the δ form can be formed, exhibits a single N^2H signal at 33.6 ppm in acetonitrile at 30 °C. This ensures us that the two N^2H signals for 3 at 40.1 and 34.7 ppm were due to the existence of two isomers.

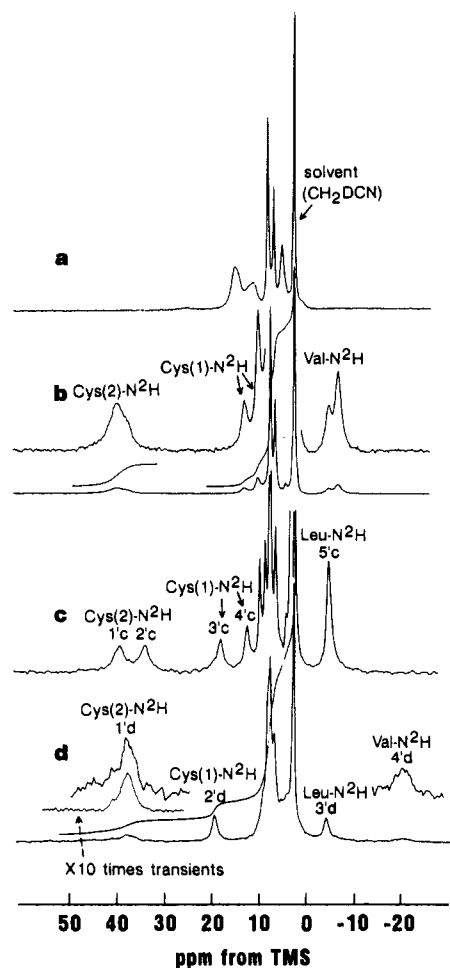


Figure 4. ^2H -NMR spectra of Cys-containing peptide Fe(II) complexes in acetonitrile at 30 °C: (a) $(\text{NEt}_4)_2[\text{Fe}^{\text{II}}(\text{Z-cys-Gly-Val-OMe})_4]$ (1); (b) $(\text{NEt}_4)_2[\text{Fe}^{\text{II}}(\text{Z-cys-Pro-Val-cys-OMe})_2]$ (2); (c) $(\text{NEt}_4)_2[\text{Fe}^{\text{II}}(\text{Z-cys-Pro-Leu-cys-OMe})_2]$ (3); (d) $(\text{NEt}_4)_2[\text{Fe}^{\text{II}}(\text{Z-cys-Pro-Leu-cys-Gly-Val-OMe})_2]$ (4).

signals were detected.²⁵ The signals due to the weak NH...S hydrogen bond at 10–20 ppm were assigned to Cys(1) N^2H *vide infra*. Thus, the signals appeared at up-field (0 to –10 ppm) were left to be assigned to Leu or Val N^2H .

Furthermore, ^2H -NMR spectra of 2 and 3 in Me_2SO are almost the same as the corresponding ones in acetonitrile. This solvent independent property was also found in CD spectra of 2 and 3 since no essential difference of the CD spectra was observed in acetonitrile and in Me_2SO . The results suggest that the two intra-ring NH (or N^2H)...S hydrogen bonds are shielded from solvent by the chelation of Cys-X-Y-Cys peptide to Fe(II) ion in complexes 2 and 3. On the other hand, $(\text{NEt}_4)_2[\text{Fe}^{\text{II}}(\text{Z-cys}(1)\text{-Pro-Leu-cys}(2)\text{-Gly-Val-OMe})_2]$ shows an additional N^2H signal at –20.0 ppm, as shown in Figure 4d. The new isotropically shifted signal at –20.0 ppm is assignable to Val N^2H , which is involved in a strong Val-NH...S-Cys(2) hydrogen bond with a β -II-like conformation of Cys-Gly-Val unit in acetonitrile. Thus, the Z-Cys-Pro-Leu-Cys-Gly-Val-OMe ligand provides three strong NH...S hydrogen bonds as shown in the schematic structure (Figure 7).

The temperature-dependence of isotropically shifted N^2H signals shown in Figure 4 was also examined. A linear relation between $\delta(\text{H})/H_0$ and $1/T$ was obtained, as shown in Figure 5.

Figure 6 shows the temperature dependence of ^1H -NMR or ^2H -NMR signals in the –25 ppm to +60 ppm region for $(\text{NEt}_4)_2[\text{Fe}^{\text{II}}(\text{Z-cys-Pro-Val-cys-OMe})_2]$ in acetonitrile- d_3 or acetonitrile.

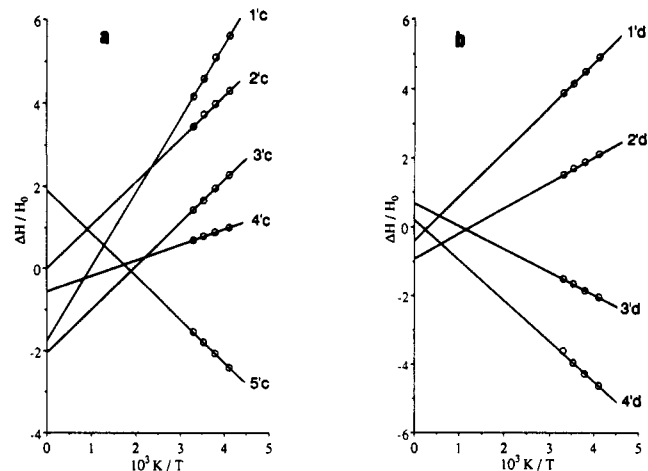


Figure 5. Curie plots against T^{-1} for the N^2H ^2H -NMR signals shown in Figure 4c,d: (a) $(\text{NEt}_4)_2[\text{Fe}^{\text{II}}(\text{Z-cys-Pro-Leu-cys-OMe})_2]$ (3); (b) $(\text{NEt}_4)_2[\text{Fe}^{\text{II}}(\text{Z-cys-Pro-Leu-cys-Gly-Val-OMe})_2]$ (4).

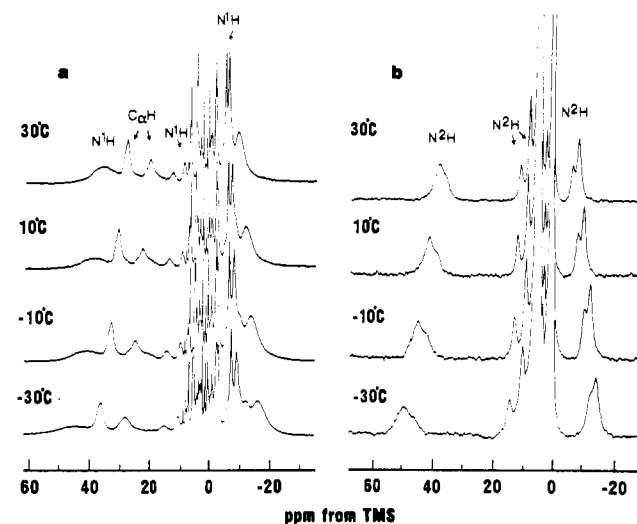


Figure 6. Temperature dependences of $(\text{NEt}_4)_2[\text{Fe}^{\text{II}}(\text{Z-cys-Pro-Val-cys-OMe})_2]$ (2): (a) ^1H -NMR signals of isotropically shifted amide NH and Cys C_αH regions in acetonitrile- d_3 ; (b) ^2H -NMR signals of the isotropically shifted amide N^2H region in acetonitrile.

Many isotropically shifted ^1H -NMR signals due to Cys C_αH and amide NH were observed in this region, while only three sets of ^2H -NMR signals due to amide N^2H were found at about 38, 11, and –6 ppm in acetonitrile at 30 °C. The corresponding ^1H -NMR signals of the amide NH protons are thus found at 36, 11, and –6 ppm in acetonitrile- d_3 at 30 °C (Table II). *D. gigas* rubredoxin showed several ^1H -NMR signals between 11 and 17 ppm in D_2O at 55 °C which were assigned to Cys C_αH protons.¹² Hence we assigned the nonexchangeable signals at 28.1 and 20.7 ppm to Cys C_αH protons (Figure 6a). The large isotropic shifts of the N^2H signals due to the amide groups of the peptide ligand are attributed to the formation of NH...S hydrogen bonds for reasons shown below.

Discussion

Chelation of Cys-Pro-Y-Cys (Y = Val, Leu) to Fe(II) Ion. Generally, the isotropic shifts follow the relationship²⁶

$$(\delta(\text{H})/H)^{\text{iso}} = \alpha T^{-1} + \beta T^{-2} \quad (1)$$

where $\alpha = -(A/h)F$ and $\beta = B(3 \cos^2 \theta - 1)r^{-3}D$. The T^{-1} dependence was attributed to the contact contribution, and the

(25) Sun, W. Y.; Ueyama, N.; Nakamura, A. Submitted for publication in *Inorg. Chim. Acta*.

(26) (a) La Mar, G. N.; Eaton, G. R.; Holm, R. H.; Walker, F. A. *J. Am. Chem. Soc.* 1973, 95, 63. (b) Bertini, I.; Luchinat, C. *NMR of Paramagnetic Molecules in Biological System*, The Benjamin/Cummings Publishing Co., Inc.: Menlo Park, CA, 1986; p 36.

Table II. Assignment of ^1H - and ^2H -NMR Hyperfine-Shifted Signals (ppm) Shown in Figure 6

NMR signal	N^1H or N^2H			Cys C_βH_2
	Cys(2)	Cys(1)	Val	
^1H	35.9	13.2, 9.6	-5.4, -8.6	28.1, 20.7
^2H	39.2, 37.2	12.4, 9.6	-5.3, -7.3	

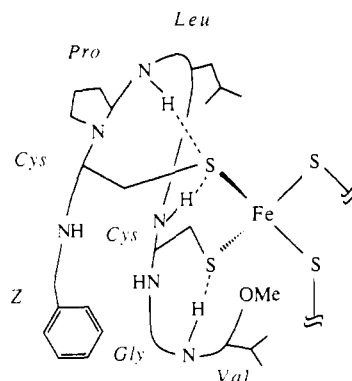
T^{-2} dependence, to the dipolar contribution. Linear $1/T$ and $\delta(\text{H})/H_0$ plots and near-zero intercepts were obtained for our peptide model complexes (Figure 3 and Table I), suggesting that the βT^{-2} term is small; i.e., the isotropic shifts of the Cys C_βH_2 are due to dominantly contact contributions through Fe-S bonds. The linear relation between $\delta(\text{H})/H_0$ of N^1H or N^2H signals and $1/T$ indicates that these N^1H or N^2H isotropic shifts are entirely contact in nature (Figures 5 and 6). The deviations from the $1/T$ axis are somewhat large, indicating perhaps partial dipolar contributions to the isotropic shifts of NH (or N^2H) since these amide NH (or N^2H) hydrogens are much closer to the iron atom than are the C_βH_2 protons.

As mentioned above, $[\text{Fe}^{\text{II}}(\text{Z-cys-Pro-Leu-cys-OMe})_2]^{2-}$ gives eight Cys C_βH_2 ^1H -NMR resonances in total (Figure 2c). In the case of $[\text{Fe}^{\text{II}}(\text{Z-cys-Pro-Val-cys-OMe})_2]^{2-}$, five Cys C_βH_2 ^1H -NMR signals were observed (Figure 2b). The peak areas of each of **1b** (**2b**), **5b** (**6b**) and **7b** (**8b**) are equal and nearly equal to the sum of signals of **3b** and **4b**. Thus, each peak of **1b** (**2b**), **5b** (**6b**) and **7b** (**8b**) is composed of two overlapping signals, and complex **2** also gives eight Cys C_βH_2 ^1H -NMR signals in total. The difference in intensities between signals **3b** and **4b** is in good agreement with the isotropically shifted N^2H signals at 40.2 and 38.3 ppm or -4.2 and -6.2 ppm (Figure 4b). The results indicate that eight Cys C_βH_2 ^1H -NMR signals of **2** and **3** are due to two diastereomers and are not due to the eight nonequivalent Cys C_βH_2 protons, which should give eight signals in the same intensity. Therefore, each isomer exhibits four Cys C_βH_2 signals; the fact that all eight Cys C_βH_2 protons are not resolved may be due to the D_{2d} symmetry as proposed by Kurtz et al.¹²

Wide separation of (a) the two groups of broad Cys C_βH_2 signals of $[\text{Fe}^{\text{II}}(\text{Z-cys-Pro-Val-cys-OMe})_2]^{2-}$ (Figure 2b) and $[\text{Fe}^{\text{II}}(\text{Z-cys-Pro-Leu-cys-OMe})_2]^{2-}$ (Figure 2-c) and (b) the four broad ones of $[\text{Fe}^{\text{II}}(\text{Z-cys-Pro-Leu-cys-Gly-Val-OMe})_2]^{2-}$ (Figure 2d) is caused by the different chemical environments of nonequivalent Cys C_βH_2 protons induced by the chelation of the Cys-X-Y-Cys fragment. The Fe(II) complex with the non-chelating peptide thiolate ligand, $[\text{Fe}^{\text{II}}(\text{Z-cys-Gly-Val-OMe})_4]^{2-}$, shows only one Cys C_βH_2 signal at 220 ppm (Figure 2a).

The relation between the Fe-S-C-H dihedral angle and the contact shifts has been discussed for 2(4Fe4S) ferredoxin²⁷ and the high-potential iron-sulfur protein (HiPIP).^{28,29} Thus, the wide separation of Cys C_βH_2 signals of complexes **2** and **3** into two groups (see Figure 2b,c: signals **1b**, **2b**, **3b**, **4b** and **5b**, **6b**, **7b**, **8b**; signals **1c**, **2c**, **3c**, **4c** and **5c**, **6c**, **7c**, **8c**) was also supposed to be caused by the different dihedral angle of Fe-S-C-H_{A or B} and may be dependent on $\cos^2 \tau$ or/and $\sin^2 \tau$ where τ is the Fe-S-C-H dihedral angle.

We have proven that the formation of NH-S hydrogen bonds causes a decrease of spin density on the sulfur atom of the cysteine residue,^{16,30} and the lower spin density makes a smaller contact shift in the ^1H -NMR spectrum.^{26b} Therefore, the signals of Cys(2) C_βH_2 should appear at relatively higher field compared to those of Cys(1) C_βH_2 in the ^1H -NMR spectrum of $[\text{Fe}^{\text{II}}(\text{Z-cys(1)-Pro-Leu-cys(2)-Gly-Val-OMe})_2]^{2-}$ due to the formation of the Val-NH-S-Cys(2) hydrogen bond. As shown

**Figure 7.** Proposed hairpin-turn-like structure of the Cys-Gly-Val fragment in complex **4**.

in Figure 2d, the signals **2d** and **4d** are at higher field than those of **1d** and **3d**. Thus, **1d**, **3d** and **2d**, **4d** were supposed to be assigned to Cys(1) C_βH_2 and Cys(2) C_βH_2 protons, respectively. The separation of **1d** and **3d** or **2d** and **4d** was also due to the different Fe-S-C-H_{A or B} dihedral angles.

NH-S Hydrogen Bonds in Cys-X-Y-Cys Chelation. Evidence for NH-S hydrogen bonding was obtained from the isotropic shifts of the amide N^2H signal using ^2H -NMR spectroscopy. The significant isotropic shifts of two sets of ^2H -NMR signals (40.1, 34.7 ppm and -4.1 ppm) assigned to Cys(2) and Leu N^2H of the Cys(1)-Pro-Leu-Cys(2) chelating ligand-Fe(II) complex (**3**) occurs through NH-S hydrogen bonds which are formed in the large macrocyclic ring. In this case, two weak isotropic shifts of N^2H signals due to Z-Cys(1) N^2H at 18.7 and 13.1 ppm are also attributed to the macrocyclic ring effect because the conformation of the macrocyclic ligands is such that Z-Cys(1) N^2H is considerably closer to other Cys(1) sulfur and forms a weak NH-S hydrogen bond. This stereochemical conclusion is supported by the BIOGRAF energy-minimum analysis on $[\text{Fe}^{\text{II}}(\text{Z-cys(1)-Pro-Leu-cys(2)-OMe})_2]^{2-}$.

Observation of the solvent-independent contact-shifted N^2H signals in $[\text{Fe}^{\text{II}}(\text{Z-cys-Pro-Leu-cys-OMe})_2]^{2-}$ indicates that these NH-S hydrogen bonds are shielded from solvent, as shown in the Cys-Pro-Leu-Cys part of the ligand (Figure 7). Similarly, the lack of a significant change in the redox potential of $[\text{Fe}^{\text{II}}(\text{Z-cys-Pro-Leu-cys-OMe})_2]^{2-}$ in Me_2SO , acetonitrile, or DME indicates that the hydrogen bonds are located inside of the macrocyclic ring and are shielded from the solvent.¹⁶

The N^2H signals were observed both upfield and downfield. This may be caused by the opposite sign of spin density, and further study on this point will be required.

Another isotropically shifted amide N^2H signal at -20.0 ppm appears in the ^2H -NMR spectrum of $[\text{Fe}^{\text{II}}(\text{Z-cys-Pro-Leu-cys-Gly-Val-OMe})_2]^{2-}$ in acetonitrile at 30 °C. Three N^2H signals (38.0, 19.5, and -4.0 ppm) of the Cys-Pro-Leu-Cys fragment definitely correspond to those (40.1, 34.7 ppm, 18.7, 13.1 ppm; and -4.1 ppm) of $[\text{Fe}^{\text{II}}(\text{Z-cys-Pro-Leu-cys-OMe})_2]^{2-}$. The isotropically shifted N^2H signal at -20.0 ppm is then assignable to Val N^2H . The value depends on the solvent used. Such a solvent dependence of the isotropic shift is in good accord with the positive shift of redox potential from -0.46 (CH₃CN) to -0.35 V vs SCE in DME.¹⁶ It has been reported that the redox potential of a metal-thiolate complex shifts to the positive side with an increase in the dielectric constant of solvent.³¹ Therefore, the positive shift in DME for $[\text{Fe}^{\text{II}}(\text{Z-cys-Pro-Leu-cys-Gly-Val-OMe})_2]^{2-}$ shows an opposite trend. The results can be explained by the presence of electrostatic interaction, that is NH-S hydrogen bonding, which is supported strongly by the nonpolar solvent. Formation of the NH-S hydrogen bond is ascribed to the conformational preference with a β -II-like hairpin

- (27) Bertini, I.; Briganti, F.; Luchinat, C.; Scozzafava, A. *Inorg. Chem.* **1990**, *29*, 1874.
 (28) Nettlesheim, D. G.; Harder, S. R.; Feinberg, B. A.; Otvos, J. D. *Biochemistry* **1992**, *31*, 1234.
 (29) Bertini, I.; Capozzi, F.; Ciurli, S.; Luchinat, C.; Messori, L.; Piccioli, M. *J. Am. Chem. Soc.* **1992**, *114*, 3332.
 (30) Ohno, R.; Ueyama, N.; Nakamura, A. *Inorg. Chem.* **1991**, *30*, 4887.

- (31) Kassner, R. J.; Yang, W. *J. Am. Chem. Soc.* **1977**, *99*, 4351.

structure of Cys-Gly-Val as described in Figure 7. This effect has already been found by two of us in the Cys-Gly-Ala fragment of $[\text{Fe}_4\text{S}_4(\text{Z-cys-Gly-Ala-OMe})_4]^{2-}$ in CH_2Cl_2 .³²

Steric Restriction for the Unique Formation of the δ Form Induced by the Gly-Val-OMe Fragment in the Z-Cys-Pro-Leu-Cys-Gly-Val-OMe/Fe(II) Complex. Steric effect caused by the peptide chelation is an important problem in metalloproteins and in their models. The stereospecificity in formation of chelating hexapeptide/Fe(II) complex is thus analyzed by the isotropically shifted peaks in its $^1\text{H-NMR}$ spectrum. Four separate Cys $\text{CH}_\text{A}\text{H}_\text{B}$ signals for $[\text{Fe}^{\text{II}}(\text{Z-cys-Pro-Leu-cys-Gly-Val-OMe})_2]^{2-}$

were observed at 257, 215, 200, and 147 ppm while the tetrapeptide Fe(II) complexes, as 2 and 3, exhibit eight signals due to presence of two isomers as mentioned above. The energy-minimized calculations for the δ and λ forms of $[\text{Fe}^{\text{II}}(\text{Z-cys-Pro-Leu-cys-Gly-Val-OMe})_2]^{2-}$ indicate considerable steric influence between the two peptide ligand chains, as shown in Figure 1. The δ form is more stable than the λ form based on the difference of ca. 16 kcal/mol in minimized total energy between the two isomers obtained using BIOGRAF. This suggests that the δ form would exist mainly in solution. The conclusion was supported by the $^2\text{H-NMR}$ results described above. Thus, steric restriction for the formation of only one isomer may be induced by oligopeptide fragments, e.g., tetra- or hexapeptide around the binding site of metal ion in rubredoxins.

(32) Ueyama, N.; Terakawa, T.; Nakata, M.; Nakamura, A. *J. Am. Chem. Soc.* **1983**, *105*, 7098.